Contract No:

This document was prepared in conjunction with work accomplished under Contract No. DE-AC09-08SR22470 with the U.S. Department of Energy (DOE) Office of Environmental Management (EM).

Disclaimer:

We put science to work.™

Savannah River National Laboratory™

OPERATED BY SAVANNAH RIVER NUCLEAR SOLUTIONS

A U.S. DEPARTMENT OF ENERGY NATIONAL LABORATORY • SAVANNAH RIVER SITE • AIKEN, SC

Nucleation and Crystal Growth Behavior of Nepheline in Simulated High-Level Waste Glasses

J.W. Amoroso

D.L. McClane

K.M. Fox

September 2017

SRNL-STI-2017-00517, Revision 0

SRNL.DOE.GOV

DISCLAIMER

Printed in the United States of America

Prepared for
U.S. Department of Energy

SRNL-STI-2017-00517
Revision 0

Keywords: *Nepheline, crystallization, growth, nucleation, DSC*

Retention: *Permanent*

Nucleation and Crystal Growth Behavior of Nepheline in Simulated High-Level Waste Glasses

J.W. Amoroso
D.L. McClane
K.M. Fox

September 2017

Prepared for the U.S. Department of Energy under contract number DE-AC09-08SR22470.

Savannah River National Laboratory™
OPERATED BY SAVANNAH RIVER NUCLEAR SOLUTIONS

REVIEWS AND APPROVALS

AUTHORS:

J.W. Amoroso, Immobilization Technology Date

D.L. McClane, Immobilization Technology Date

K.M. Fox, Wasteform Processing Technology Date

TECHNICAL REVIEW:

F.C. Johnson, Immobilization Technology, Reviewed per E7 2.60 Date

APPROVAL:

C.C. Herman, Director
Wasteform Processing Technology Date

ACKNOWLEDGEMENTS

The authors thank Mark Reboul, Anthony McWilliams, David Missimer, Phyllis Workman, Madison Caldwell, Kim Wyszynski, Beverly Wall, and Whitney Riley at Savannah River National Laboratory for their assistance with the laboratory analyses described in this report. Funding for this work by the U.S. Department of Energy Office of River Protection Waste Treatment & Immobilization Plant Project through Inter-Entity Work Order M0SRV00101 managed by Albert A. Kruger is gratefully acknowledged.

EXECUTIVE SUMMARY

The Savannah River National Laboratory (SRNL) has been tasked with supporting glass formulation development and process control strategies in key technical areas, relevant to the Department of Energy's Office of River Protection (DOE-ORP) and related to high-level waste (HLW) vitrification at the Waste Treatment and Immobilization Plant (WTP). Of specific interest is the development of predictive models for crystallization of nepheline ($NaAlSiO_4$) in HLW glasses formulated at high alumina concentrations. This report summarizes recent progress by researchers at SRNL towards developing a predicative tool for quantifying nepheline crystallization in HLW glass canisters using laboratory experiments.

In this work, differential scanning calorimetry (DSC) was used to obtain the temperature regions over which nucleation and growth of nepheline occur in three simulated HLW glasses - two glasses representative of WTP projections and one glass representative of the Defense Waste Processing Facility (DWPF) product. The DWPF glass, which has been studied previously, was chosen as a reference composition and for comparison purposes. Complementary quantitative X-ray diffraction (XRD) and optical microscopy confirmed the validity of the methodology to determine nucleation and growth behavior as a function of temperature.

The nepheline crystallization growth region was determined to generally extend from ~ 500 to >850 °C, with the maximum growth rates occurring between 600 and 700 °C. For select WTP glass compositions (high Al_2O_3 and B_2O_3), the nucleation range extended from ~ 450 to 600 °C, with the maximum nucleation rates occurring at ~ 530 °C. For the DWPF glass composition, the nucleation range extended from ~ 450 to 750 °C with the maximum nucleation rate occurring at ~ 640 °C. The nepheline growth at the peak temperature, as determined by XRD, was between 35 - 75 wt.% /hour. A maximum nepheline growth rate of ~ 0.1 mm/hour at 700 °C was measured for the DWPF composition using optical microscopy.

This research establishes a viable alternative to more traditional techniques for evaluating nepheline crystallization in large numbers of glasses, which are prohibitively time consuming or otherwise impractical. The ultimate objective is to combine the nucleation and growth information obtained from DSC, like that presented in this report, with computer simulations of glass cooling within the canister to accurately predict nepheline crystallization in HLW during processing through WTP.

TABLE OF CONTENTS

LIST OF TABLES

LIST OF FIGURES

LIST OF ABBREVIATIONS

CCC	Canister centerline cooling
DOE	U.S. Department of Energy
DSC	Differential Scanning Calorimetry
DWPF	Defense Waste Processing Facility
HLW	High-level waste
LAW	Low-activity waste
ORP	Office of River Protection
PCT	Product Consistency Test
SEM	Scanning Electron Microscopy
SRNL	Savannah River National Laboratory
TTQAP	Task Technical and Quality Assurance Plan
WTP	Waste Treatment and Immobilization Plant
XRD	X-Ray Diffraction

1.0 Introduction

The U.S. Department of Energy (DOE) Office of River Protection (ORP) plans to process 55 million gallons of radioactive waste stored at the Hanford Site in Washington through the Waste Treatment and Immobilization Plant (WTP). Low-activity waste (LAW) accounts for ~90% of the tank waste as liquid supernatant while the remaining solids and heavy precipitates comprise the high-level waste (HLW) fraction. Both LAW and HLW will ultimately be vitrified into borosilicate glass.[1]

DOE-ORP has requested that the Savannah River National Laboratory (SRNL) support glass formulation development and process control strategies in key technical areas, related to glass formulation development for WTP and as defined in the Task Technical and Quality Assurance Plan (TTQAP).[2] One of the technical areas is the development of predictive models for crystallization of nepheline ($NaAlSiO_4$) in HLW glasses formulated at high alumina concentrations. Progress in this area should enable increases in loading of Hanford tank wastes in glass while maintaining the ability to meet processing, regulatory compliance, and product quality requirements.

The performance of HLW glass can be quantified by its resistance to aqueous chemical degradation, or durability, as measured by the ASTM Product Consistency Test (PCT).[3] The PCT response is generally determined by the glass composition, but crystalline phases that form during processing, such as nepheline, are known to adversely affect the PCT response.[4,5] Crystallization in HLW occurs during the vitrification process in which the melted glass (waste feed in combination with additives) is poured into stainless steel canisters and allowed to cool in ambient air.[3] Because the volume of poured glass is large, it can take >24 hours for the poured glass to cool, during which time crystallization may take place if the composition is not controlled. WTP will fill canisters using successive batch pours, or lifts, in which molten glass will be poured onto partially cooled glass. During a successive pour, some volume of glass near the contact interface, will experience a thermal history that should theoretically amplify the crystallization potential in the glass. The ability to predict the formation of nepheline in a WTP canister as a function of glass composition will allow WTP to maximize waste loading in glass while maintaining acceptable durability.

This report summarizes recent progress by researchers at SRNL towards developing a predictive tool for quantifying nepheline crystallization in HLW glass canisters using laboratory experiments. In this work, differential scanning calorimetry (DSC) is used to obtain the temperature ranges over which nucleation and growth of nepheline occur in simulated HLW glasses. The work presented here establishes the methodology as a viable alternative to more traditional techniques, such as developing time-temperature-transformation (TTT) curves, which are typically prohibitively time consuming or otherwise impractical for evaluating large numbers of glasses. The ultimate objective is to combine the nucleation and growth information obtained from DSC, like that presented in this report, with computer simulations of glass cooling within the canister to accurately predict nepheline crystallization in HLW during processing through WTP. As will be shown, the results of this research can now be combined with previous modeling efforts developed at SRNL[6] to meet this objective.

2.0 Experimental Procedure

2.1 Composition Selection

Three glass compositions were selected for this study, based on high aluminum concentration waste feeds. Two compositions were selected from a Pacific Northwest National Laboratory (PNNL) study and are intended to be prototypic of a WTP HLW glass. One composition was selected from a SRNL study and is prototypic of a Defense Waste Processing Facility (DWPF) HLW glass. The two compositions from the PNNL study exhibit different amounts of nepheline crystallization, but similar type and amounts of secondary crystalline phases after the WTP canister centerline cooled (CCC) heat treatment.[7] The SRNL composition is known to precipitate similar crystalline phases after the DWPF CCC.[8] Table 1 and Table 2 list published information regarding the crystallization behavior of the glasses and their target oxide compositions, respectively. Figure 1 depicts the normalized ternary compositions based on the primary components (SiO_2-Na_2O-Li_2O-Al_2O_3-B_2O_3) of each glass composition and overlaid on the Na_2O-SiO_2-Al_2O_3 equilibrium phase diagram.

Table 1. Vital statistics of test glasses from published sources.

Glass ID	Heat Treatment	Nepheline (wt.%)	Other, Crystalline Phase, (powder diffraction file #), wt.%
NP2-Low-Li[7]	WTP CCC	1.8	Lithium Iron Oxide (51206), 2.6 Lithium Iron Manganese Oxide (93817), 1.1
	Quenched	No data available	
NP-MC-BNA-1[7]	WTP CCC	67	Lithium Iron Oxide (155029), 2.9 Lithium Iron Manganese Oxide (93823), 1.3
	Quenched	3.1	Lithium Iron Manganese Oxide (150247), 1.8 Iron Oxide (35643), 1.1
NP2-23[8]	DWPF CCC	5.6	None
	Quenched	0.0	None

2.2 Glass Fabrication

Feedstock of the three glasses, hereafter referred to as NP2-Low-Li, NP-MC-BNA-1, and NP2-23 was prepared by combing stoichiometric amounts of reagent grade oxides, carbonates, H_2BO_3, Na_2SO_4, NaF, Na_3PO_4, and $RuCl_3$ (to obtain the target glass compositions listed in Table 2) in a 90% platinum/10% rhodium (Pt/10Rh) crucible, heated at ~1200 °C for 1 hour and water quenched. Subsequently, the quenched glass was ground in an Angstrom ring pulverizer with tungsten carbide inserts, re-melted at ~1200 °C for 1 hour in Pt/10Rh, and again quenched in water. The resulting glasses were stored as feed stock for subsequent analyses and testing.

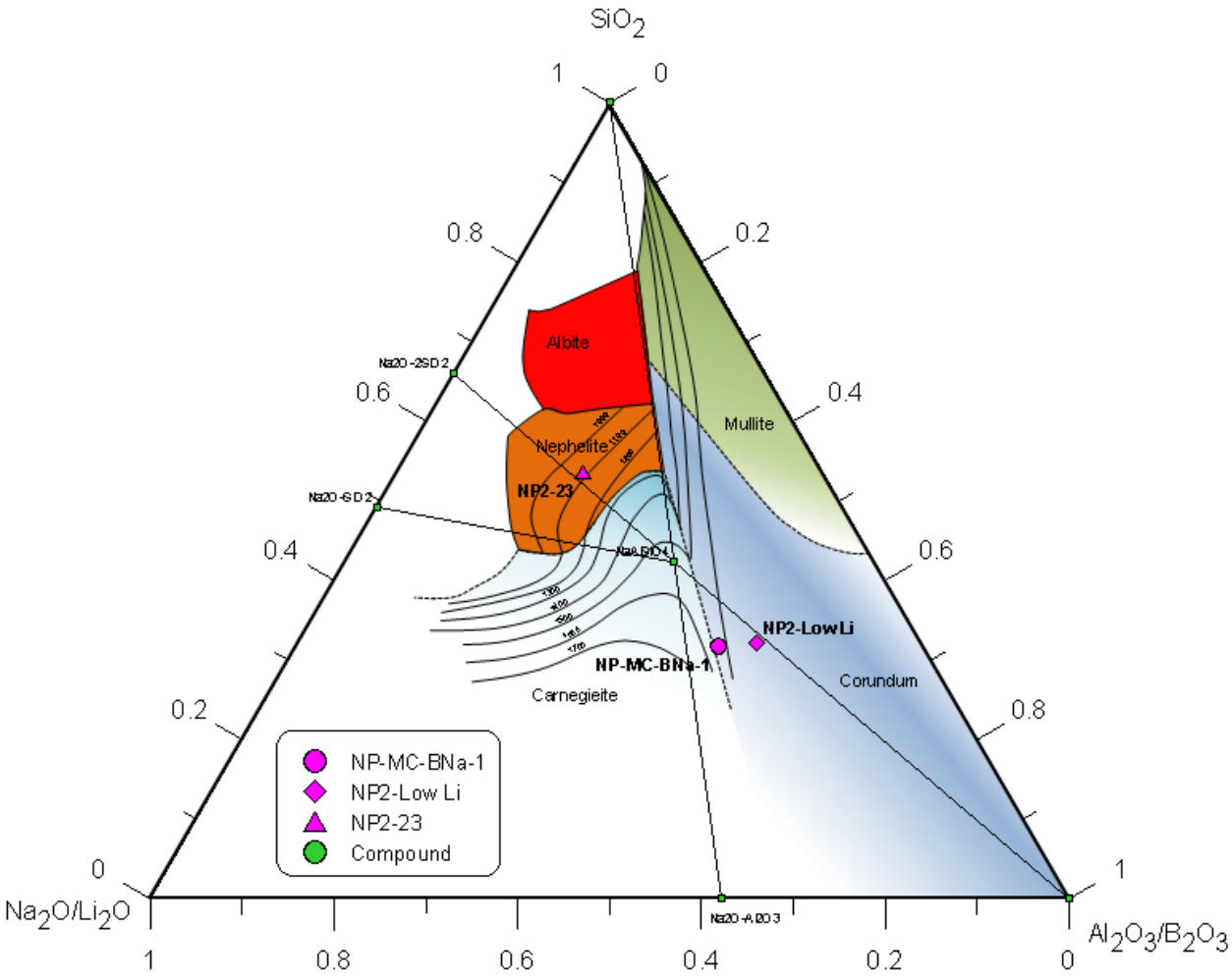

Figure 1. Phase diagram depicting the primary compositional differences of the test glasses. Dashed lines indicate estimated phase boundaries.

Table 2. Target oxide chemical composition of test glasses.

Oxide	NP2-23	NP2-Low Li	NP-MC-BNa-1
Al_2O_3	12.28	28.80	28.58
B_2O_3	4.50	17.38	14.00
Bi_2O_3	-	0.66	0.65
CaO	4.00	0.66	0.65
Cr_2O_3	0.20	1.11	1.10
F	-	0.30	0.30
Fe_2O_3	7.22	2.53	2.51
Li_2O	4.00	4.00	5.01
MgO	1.50	-	-
MnO	1.19	1.01	1.00
Na_2O	18.00	12.63	15.50
NiO	0.17	-	-
P_2O_5	-	0.71	0.70
RuO_2	-	0.05	0.05
SiO_2	44.94	29.66	29.43
SO_4	-	0.30*	0.30*
TiO_2	2.00	-	-
ZrO_2	-	0.25	0.25

* Values are reported for SO_3. Values have been converted to SO_4 for consistency throughout the document.

2.3 Methodology for Quantifying Crystallization Behavior

2.3.1 Differential Scanning Calorimetry

Differential scanning calorimetry (DSC) was used to obtain crystal nucleation-like and growth-like behavior as a function of temperature for each glass.[1] Measurements were performed on bulk and powder samples, in flowing argon (40 ml/min) with Pt/Rh pans, using a Netzsch 404 F1 Pegasus DSC. Although the methodology used is described elsewhere [9,10], a summary is provided here. In the most basic scenario, a glass sample is heated from room temperature to its nominal melting temperature to establish a baseline crystallization exotherm. Subsequent glass samples are then heated and held isothermally at specific temperatures based on the crystallization exotherm. Growth-like rate curves are obtained via differences in the integrated area ($A_o - A$) under the exotherm. Nucleation-like rate curves are obtained utilizing the shift in the exotherm peak temperature ($\frac{1}{T_p} - \frac{1}{T_{p_o}}$). Through a series of heat treatments and analysis of the crystallization exotherm for a single composition, rate-like curves as a function of temperature can be constructed.

2.3.2 X-ray Diffraction

X-ray diffraction (XRD) was used to (1) validate the DSC results and (2) quantify the crystallization in glass samples as a function of treatment temperature. Samples were initially ground in an automatic Spex mill for 4 minutes. Subsequently, the powders were hand ground in agate with alcohol and mounted to a glass slide using a collidion/Amyl Acetate solution. The measurement conditions provided a 0.5 wt%

[1] The curves are "like" because they are not directly measured but instead are derived from relative changes in heat flow among heat treated samples and correlated to crystallization phenomena.

detection limit, meaning that if a crystal phase was present at this concentration (or greater), the type of crystal(s) (or phase) could be identified. It follows that if a characteristically broad hump(s) is measured, then the sample is considered X-ray amorphous under the measurement conditions.

2.3.3 Microscopy

Although XRD can be used to quantify total crystal content, it cannot be used to investigate nucleation rates or crystal growth rates directly. Electron and optical microscopy were used to (1) validate the DSC results and (2) elucidate nucleation and crystallization behavior. One glass, NP2-23, was selected for optical characterization. Thin sections (~0.5 mm) were cut from heat treated bulk samples (~1 x 1 x 0.5 cm). The thin sections were given a final surface polish using 2800 grit SiC paper and were examined for crystallization, homogeneity, and overall visible appearance using an Olympus SZX16 stereo microscope for low magnification imaging. Routine phase identification and imaging was performed using a Hitachi TM3000 scanning electron microscope (SEM).

2.4 Analyses

2.4.1 Chemical Composition

Each glass feed stock was sampled and analyzed chemically to confirm that the as-fabricated glasses met the target compositions. Two digestion methods, sodium peroxide fusion (PF) and lithium-metaborate fusion (LM), were used to prepare samples for cation measurements. Each glass was prepared in duplicate for each of the dissolution techniques. All of the prepared samples were analyzed for each element of interest by Inductively Coupled Plasma – Atomic Emission Spectroscopy (ICP-AES). The instrument was calibrated using NIST traceable standards and verified using a glass standard. Check standards were measured after the calibration, in between dilutions, and after the last sample to ensure the performance of the ICP-AES over the course of the analysis. The measured cation concentrations were converted to their respective oxides to obtain a wt.% of each component oxide and are listed in Table 3.

Table 3. Measured compositions of the test glasses.

	NP2-23	NP2-Low Li	NP-MC-BNa-1
Al_2O_3	12.3	29.1	26.9
B_2O_3	5.0	17.4	13.8
Bi_2O_3	-*	n.m.†	0.6
CaO	4.4	0.6	0.6
Cr_2O_3	0.2	0.9	1.0
F	-	n.m.	n.m.
Fe_2O_3	7.4	2.6	2.4
Li_2O	4.3	4.1	4.6
MgO	1.4	-	-
MnO	1.3	0.9	0.9
Na_2O	18.8	12.1	14.8
NiO	0.2	-	-
P_2O_5	-	0.8	0.5
RuO_2	-	<0.1	<0.01
SiO_2	45.5	32.7	31.3
SO_4	-	0.3	0.3
TiO_2	2.1	-	-
ZrO_2	-	0.2	0.2

* "-" indicates no addition of element/oxide to batch.
† "n.m." indicates the element was not measured.

3.0 Quality Assurance

Requirements for performing reviews of technical reports and the extent of review are established in manual E7 2.60. SRNL documents the extent and type of review using the SRNL Technical Report Design Checklist contained in WSRC-IM-2002-00011, Rev. 2.

4.0 Results and Discussion

4.1 Methodology for Quantifying Crystallization Behavior

4.1.1 Differential Scanning Calorimetry

DSC measurements were performed using a sieved fraction of crushed glass, -200 to +400 mesh (37 -74 μm).[2] A 20 K/min ramp rate was utilized to reach each hold temperature. Samples were then isothermally held at this temperature for 30 minutes and cooled at 20 K/min to 150 °C.[3] Samples were held at 150 °C for 15 minutes to allow for equilibration of the temperature and subsequently heated at 20 K/min to temperatures in excess of 1000 °C. A representative heat treatment is shown in Figure 2, the resulting DSC spectra obtained for heat treating NP2-23 at various temperatures is shown in Figure 3. The spectra are overlaid to show the representative shift in position and changes to the area of the exothermic peaks used to calculate nucleation and growth temperatures.

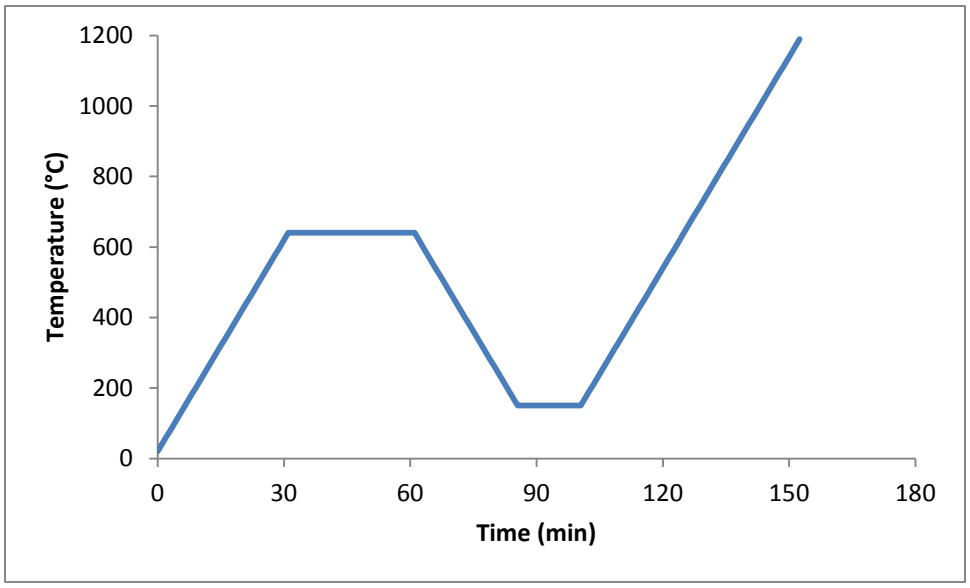

Figure 2. Representative DSC Heat Treatment

[2] See Section 4.2 for discussion of the effects of particle size (i.e., sieve fraction) on the DSC signal and crystallization behavior.
[3] This step was not performed for the samples that had a target hold temperature of 150°C.

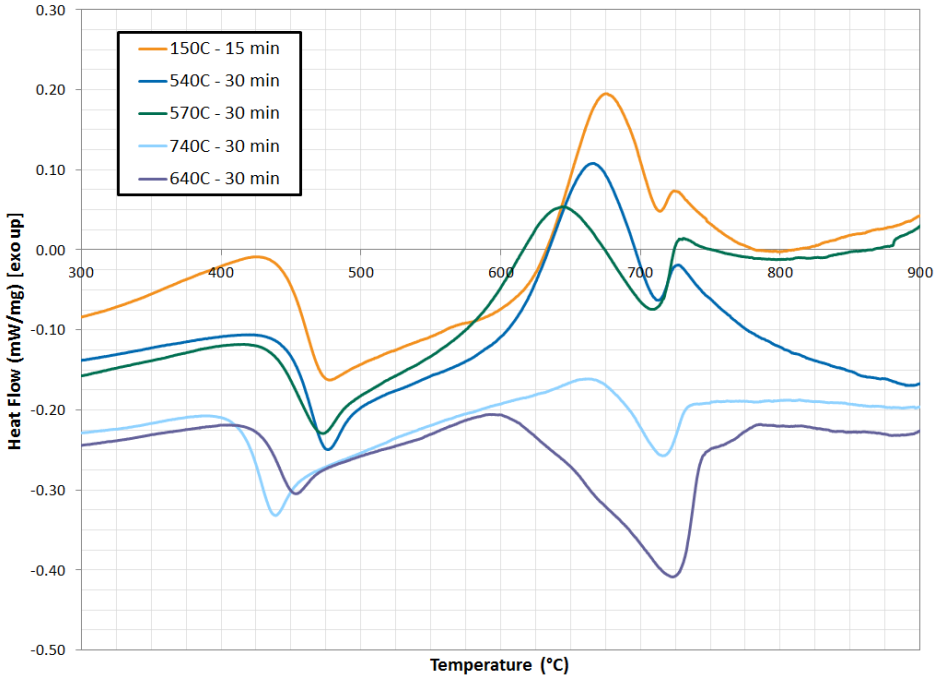

Figure 3. Example DSC curves for NP2-23 showing exotherm peak temperature and area following isothermal heat treatment.

The resulting nucleation-like and growth-like curves obtained from tracking changes to the exothermic peaks in the DSC signal changes after isothermal heat treatments are shown in Figure 4 for each glass. In Figure 4, polynomial fits to the data have been drawn to aid in visualizing the growth-like curves whereas a Guassian function was fit to the nucleation-like curves. Overlap in the temperature range for nucleation and growth is evident in all three of the glass compositions studied. The nucleation and growth temperatures overlap almost entirely for the NP2-23 glass. Although nucleation and growth temperatures partially overlap in the NP2-Low-Li and NP-MC-BNA-1 glasses, the maximum temperatures for nucleation and growth are separated by >75 °C in those glasses.

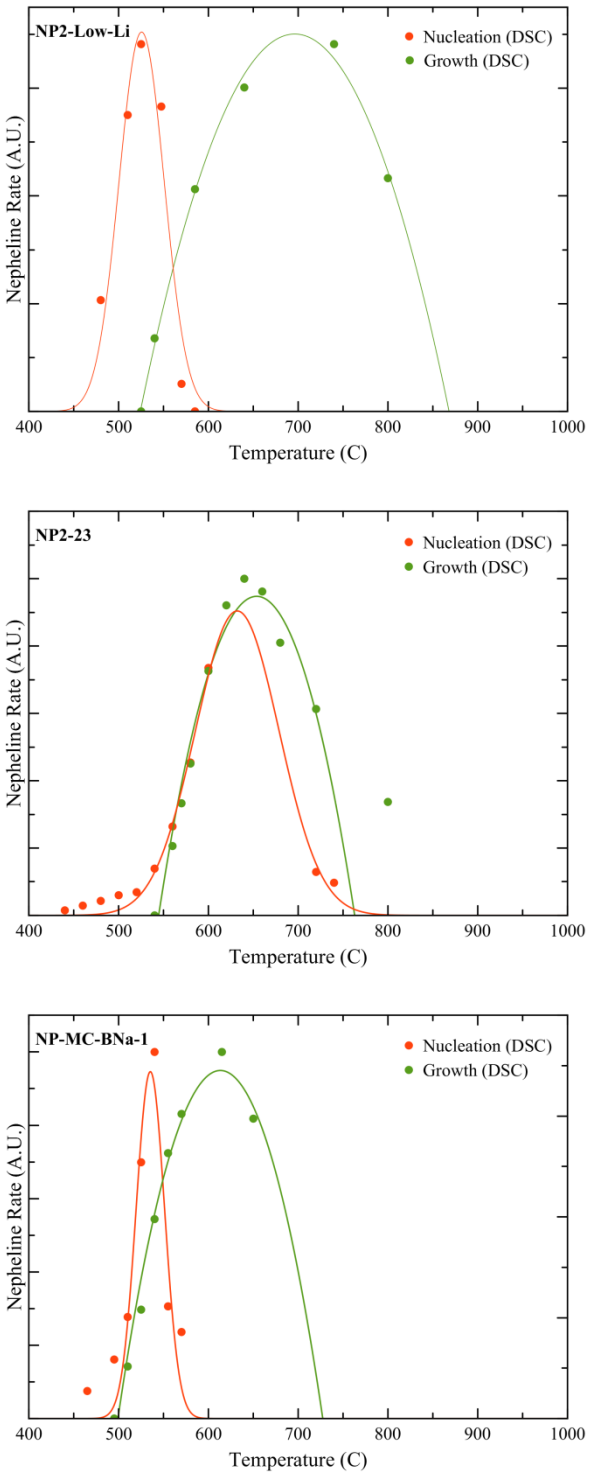

Figure 4. Nucleation-like and growth-like curves for the three test glasses based on DSC analysis.

4.1.2 X-Ray Diffraction

Based on the nucleation-like and growth-like curves, a larger volume of material was heated in a laboratory furnace to simulate the DSC heat treatments and analyzed with XRD to quantitatively determine the types and amounts of crystalline phases. Approximately 3g of the -200/+400 mesh powder, in a 1 x 1 x 0.5-inch Pt/10Rh pan, was used per heat treatment sample. Samples were placed in a pre-heated furnace and air quenched after isothermal holds. Figure 5 shows representative diffraction patterns collected for glasses heat treated for ~ 30 min. at varying temperatures. Nepheline was identified as a primary phase in all samples. A lithium manganese iron oxide phase, believed to represent more generally spinel, was identified as a secondary phase in all glasses, which was reported previously for the NP2-Low-Li and NP-MC-BNa-1 glasses.[4][7] A minor lithium silicate phase was also identified in the NP2-23 sample. The quantitative XRD results for ~30-minute isothermal growth temperatures based on the DSC curves are listed in Appendix A.

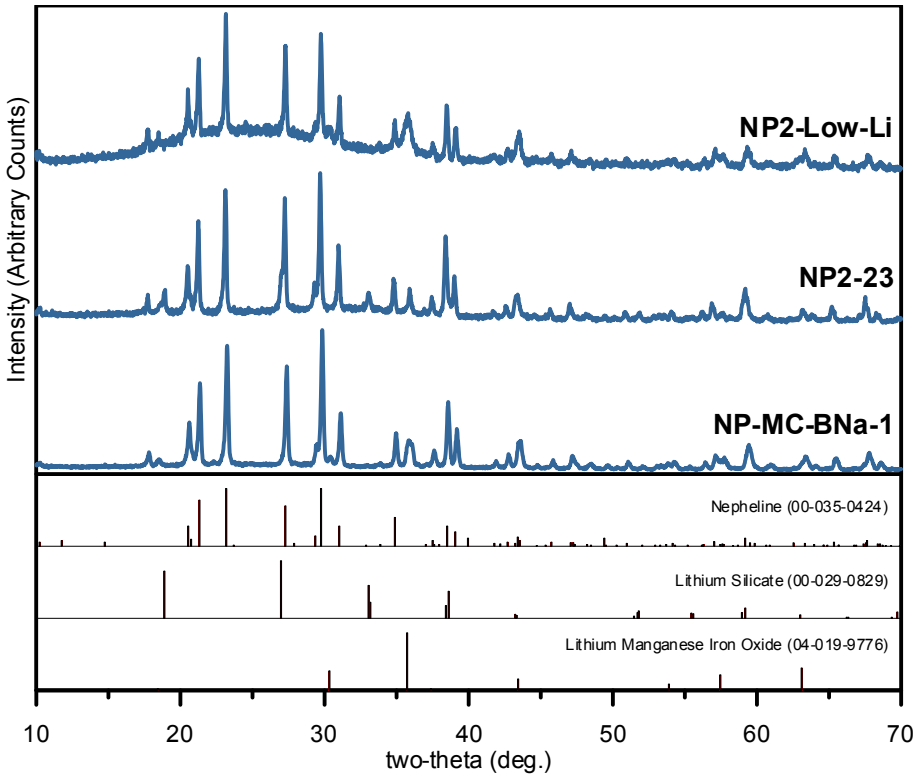

Figure 5. XRD of test glasses after heat treatment. (NP2-Low-Li – 646 °C, 36 minutes; NP2-23 – 645 °C, 31 minutes; NP-MC-BNa-1 – 611 °C, 30 minutes). Patterns used for quantitative phase analysis are shown under the spectra.

The measured nepheline concentration, as a function of temperature and divided by the isothermal growth time (e.g., ~30 minutes), is overlaid with the DSC nucleation-like and growth-like curves in Figure 6. In Figure 6, the nucleation and growth curves based on the DSC data are scaled to match the growth rate calculated from the XRD data. The resulting plots show excellent agreement with the temperature region of growth determined using DSC. These XRD results broadly represent the total wt.% nepheline growth per hour for each glass composition in the test matrix. Examination of the growth rates indicates that

[4] The spinel phase, which was not previously detected by XRD in the NP2-23 glass, is believed to have been below the detection limit due to the lower surface area to volume ratio used in that study which, as will be discussed later, results in less total spinel (because it nucleates and grows primarily at the surface in the NP2-23 glass)

composition can significantly affect the maximum nepheline growth rate temperature and, to a lesser extent, the nepheline growth temperature range. This is particularly interesting considering that the minor compositional differences between the NP2-Low-Li and NP-MC-BNa-1 glasses amount to a difference in the maximum nepheline growth rate temperature of 50 – 100 °C.

In summary, the results presented indicate the usefulness of using DSC to predict temperature regions over which nepheline crystallization will occur. These results do not explicitly consider effects such as changing surface area (as the glass powder melts) or convoluted nucleation and growth of new crystals as compared to ideal devitrification transformation caused by crystal growth. Therefore, further experiments were conducted to elucidate the crystallization behavior.

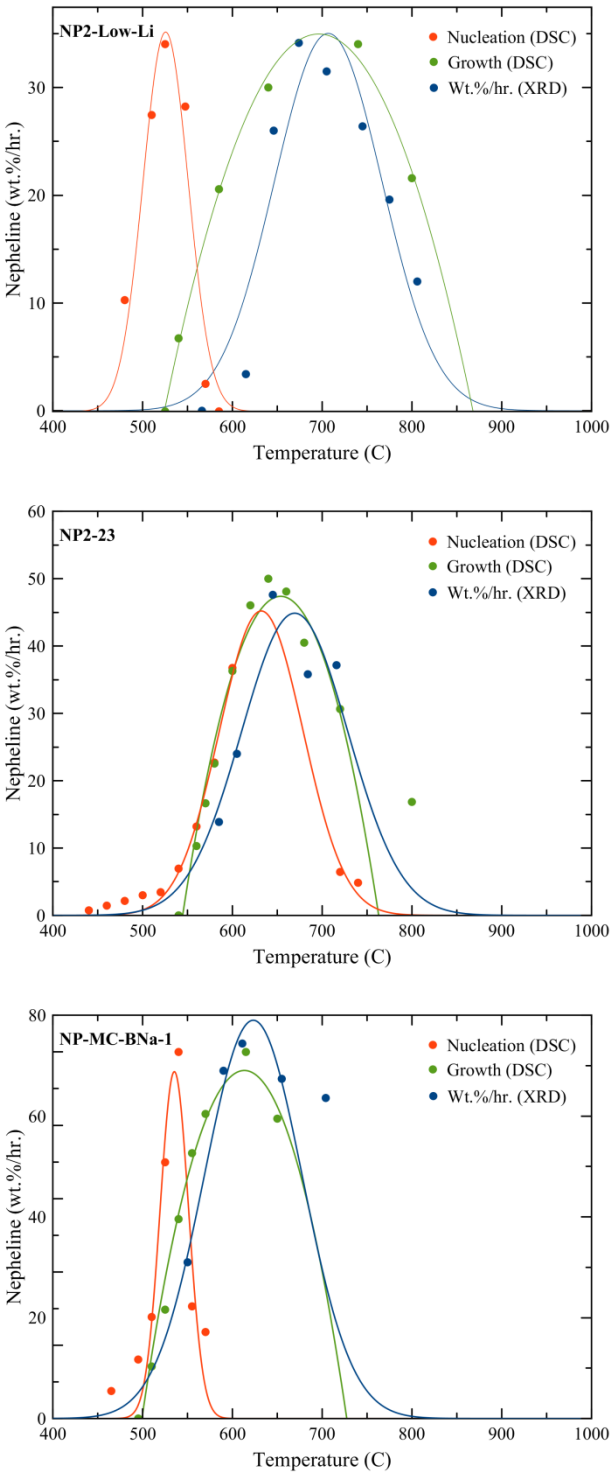

Figure 6. Normalized nepheline growth rates (wt.%/hr.) as measured by XRD overlaid with nucleation and growth rate curves for the three test glasses based on DSC analysis.

4.1.3 Optical Microscopy

To further investigate the crystallization behavior, bulk samples (~3g) of the NP2-23 feedstock glass were heat treated in a laboratory furnace and subsequently analyzed with optical microscopy. Samples were equilibrated at ~1200 °C for ~1 hour and subsequently transferred to a pre-heated furnace set at the desired temperature for a set amount of time. Figure 7 shows an image of a cross section of NP2-23 isothermally held at 700 °C for 8 hours. In Figure 7, surface crystallization appears to dominate the growth behavior. Crystal habit was used to identify nepheline as the hexagonal prisms (appearing as rectangles when positioned on edge face) visible as discrete crystals in the bulk and forming a uniform layer at the surface. Phase contrast imaging using SEM was insufficient to distinguish between nepheline and the glass matrix (~ identical Z contrast); however, energy dispersive spectroscopy (EDS) indicated areas rich in Na and Al corresponding to the surface layer thickness.

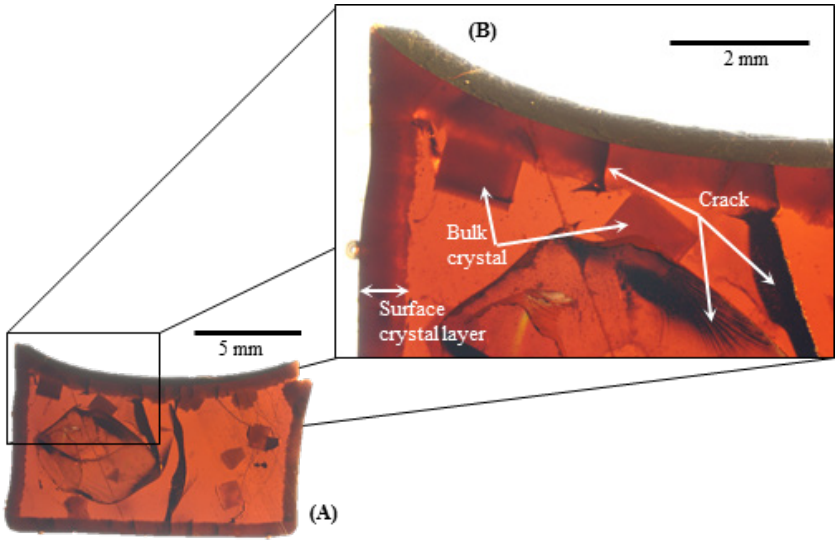

Figure 7. Optical image of NP2-23 glass heat treated at 700 °C for 8 hours showing (A) the full polished cross-section and (B) and magnification of the surface crystal layer.

Two-step isothermal heat treatments, based on the DSC results, were used to systematically investigate the nucleation and growth behavior in the NP2-23 glass further. In one set of experiments, the glasses were held at a nucleation temperature of 570 °C for 10 minutes, followed by isothermal heat treatment at 620 °C for 2, 4, 8, 18, and 24 hours. A second set of glasses was held at a nucleation temperature of 570 °C for 10 minutes, followed by isothermal heat treatment for 4 hours at 620, 640, 660, 700, and 760 °C. The nucleation step was performed to impart a nominal nuclei concentration in all the glasses prior to the growth temperature step. In both types of measurements, the glasses were first equilibrated at 1200 °C for ~1 hour and transferred (while hot) to a pre-heated furnace for the subsequent heat treatment steps.

Images, taken using transmitted light, of cross sections of the heat-treated glasses are shown in Figure 8 and Figure 9. In those images, it is clear that surface crystallization dominated the growth behavior in all samples. In Figure 8, crystal size increases with time and is accompanied by a negligible change in the number of crystals. In Figure 9, the number of crystals increased to a maximum at 660 °C and then decreased at higher temperatures. A noticeable increase in crystal size was visible up to 700 °C. Taken together, the results support the DSC and XRD results indicating that nucleation and growth occur simultaneously in the NP2-23 glass composition at temperatures below 660 °C, the nucleation rate

decreases significantly at ~700 °C, and growth dominates the behavior until its rate also decreases at ~760 °C.

A crystal growth rate was also determined for NP2-23 by measuring the thickness of the surface layer on a number of heat treated glasses and calculating the growth rates, in mm/hour. The crystal thickness layer plotted as a function of time is shown in Figure 10. Linear fits to the data in Figure 10 indicate a linear dependence for the growth rate, which is further indication that surface crystallization dominates the behavior in the NP2-23 glass.[11] For the temperatures measured, averages of the developed crystal layer thickness are plotted over varying times in Figure 11. The growth rate curve measured using optical microscopy is shifted to a higher temperature than that measured using DSC or XRD. The difference can be understood be recalling that although the peak nucleation and growth temperatures regions overlap, the growth region is (and will) have greater magnitude at higher temperatures compared to the nucleation region. It follows that although the nepheline crystal size increases to a maximum at ~720 °C, the greatest total wt.% of nepheline occurs at a lower temperature, ~640 °C.

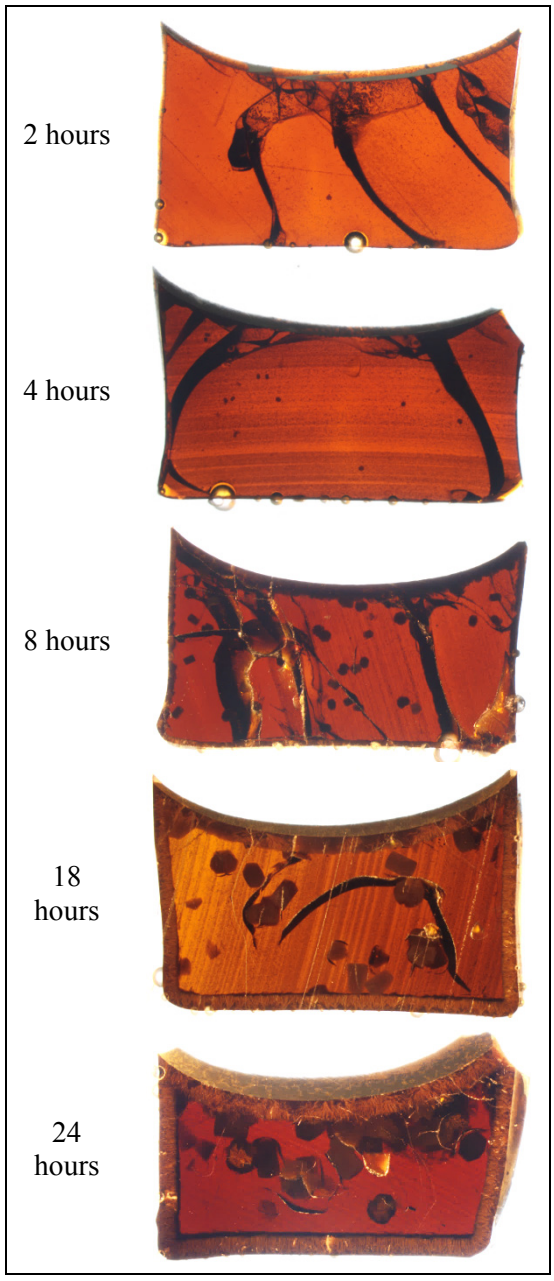

Figure 8. Crystals grown in NP2-23 glass at 620 °C for 2, 4, 8, 18, and 24 hours following 10-minute nucleation step at 570 °C.

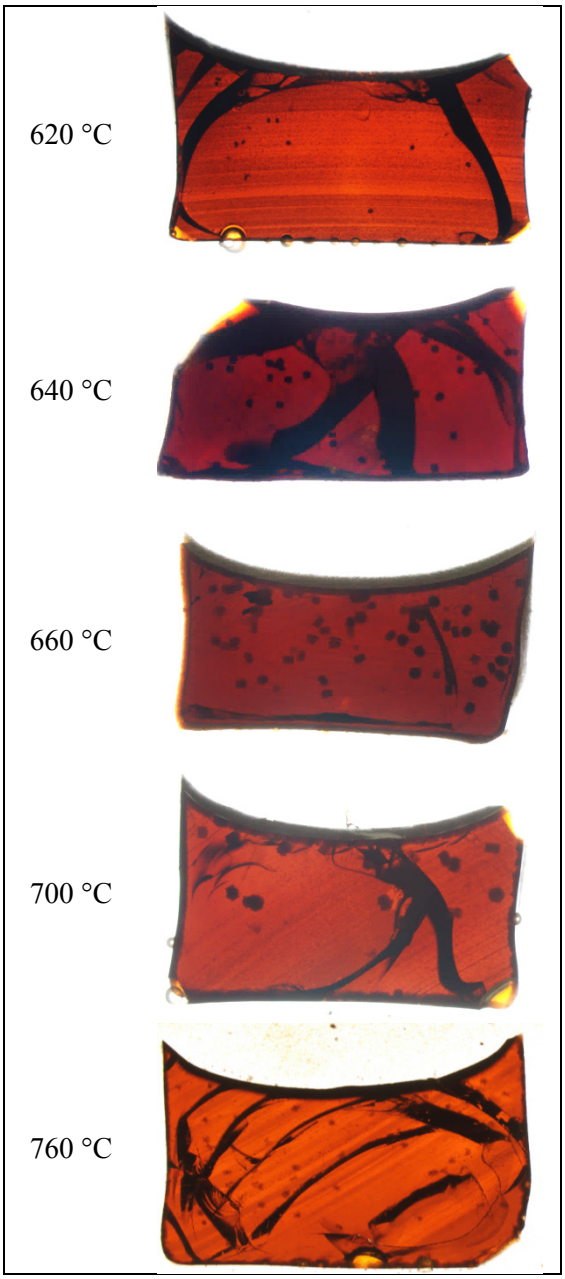

Figure 9. Crystals grown in NP2-23 glass for 4 hours at 620, 640, 660, 700, and 760 °C following a 10-minute nucleation step at 570 °C.

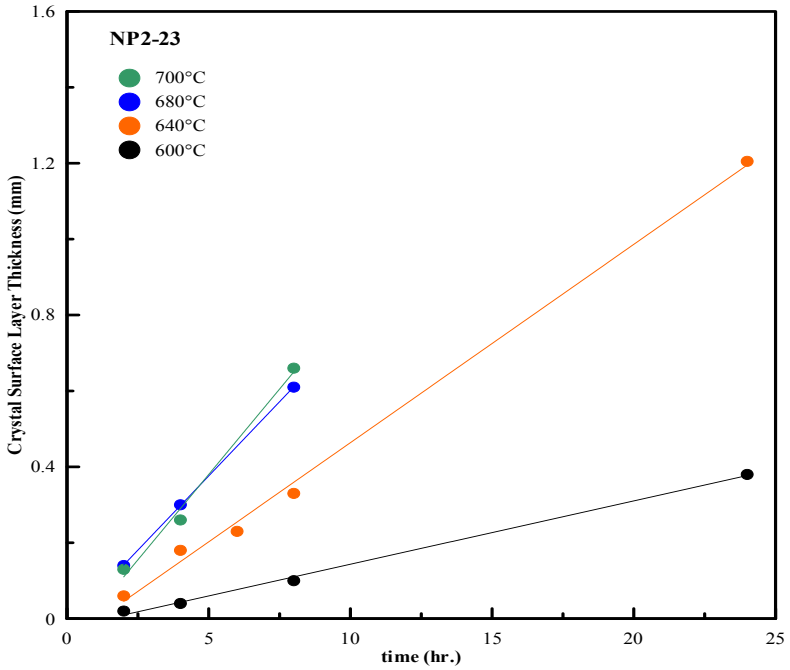

Figure 10. Crystal surface layer thickness as a function of time for various isothermal heat treatment temperatures for NP2-23.

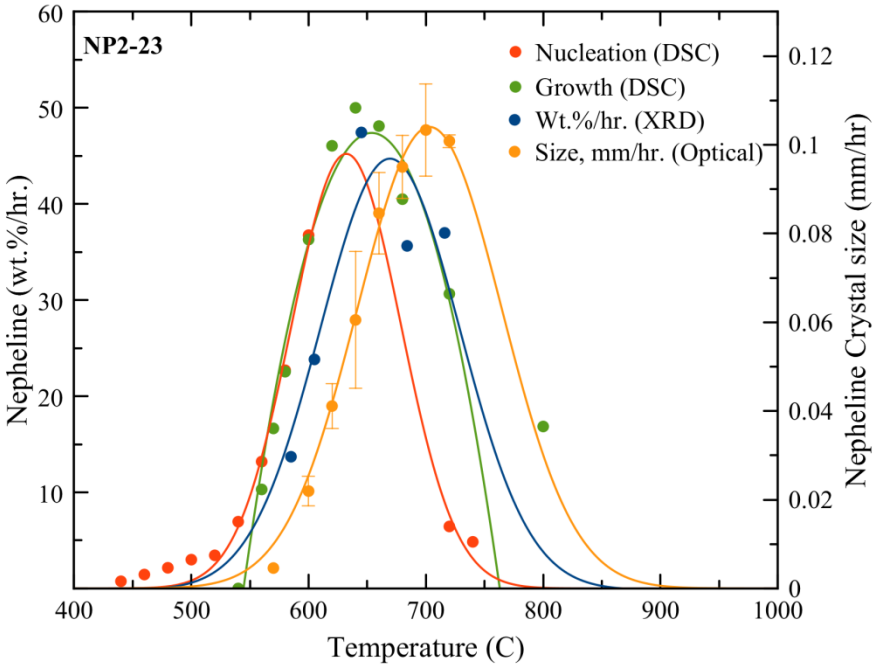

Figure 11. Average nepheline growth rates (mm/hour) as measured by optical microscopy and overlaid with nucleation and growth curves (A.U.) for the NP2-23 glass obtained from DSC analysis. Error bars are calculated as the standard deviation of rates determined per temperature (usually 2-3 different isothermal hold times).

4.2 Surface versus bulk crystallization

It has been shown in the NP2-23 glass composition, and has been previously reported for a number of HLW glasses[8], that nepheline primarily grows from the surface. Understanding whether nepheline grows primarily in the bulk or at the surface is critical to developing a predictive tool and representative laboratory experiments. More importantly, it is important to understand bulk and surface nepheline crystal growth in HLW glass because the amount of nepheline that precipitates in HLW glass during processing can vary significantly, depending on the type of crystal growth. To investigate this phenomenon further, samples of the test glasses were prepared with intentionally varied surface area to volume ratios and analyzed using DSC.

For each glass, three ground and sieved particle sizes were heated in the DSC at a rate of 20 K/min to obtain baseline DSC curves. The particle sizes were +35 mesh (>500 μm), -100/+200 mesh (74-150 μm), and -200/+400 mesh (37-74 μm). The resulting DSC curves are shown in Figure 12, Figure 13, and Figure 14, respectively. In these figures, an ideal bulk crystallization event would be expected to not change position (temperature) or intensity as a function of particle size, whereas the opposite would be expected for a surface crystallization event.

Bulk crystallization behavior is evident in the spectra measured for the NP-Low-Li glass (Figure 12), in which a consistent peak at ~650 °C is seen in all spectra and is accompanied by an emergent peak with increasing surface area at ~750 °C. The second peak is thought to be associated with surface crystallization.

The NP2-23 glass, which has been shown to be dominated by surface crystallization (Section 4.1.3), exhibited an opposite trend, as expected. The NP2-23 spectra (Figure 13) reveal a peak at ~715 °C that decreases in intensity with increasing particle size and is accompanied by the emergence of a second peak at ~850 °C, concealed by the tail of the significantly more intense peak at the lower temperature. There is some peak shifting associated with the lower temperature peak that may be due to nucleation, as was shown to occur simultaneously with the growth.

Interpretation of the spectra associated with the NP-MC-BNa-1 glass (Figure 14) is more difficult. The behavior appears to be similar to that of NP2-23 but the spectra are more complex. Nevertheless, there appears to be surface and bulk crystallization simultaneously, likely somewhere in between that of what is observed in NP2-23 and NP2-Low-Li.

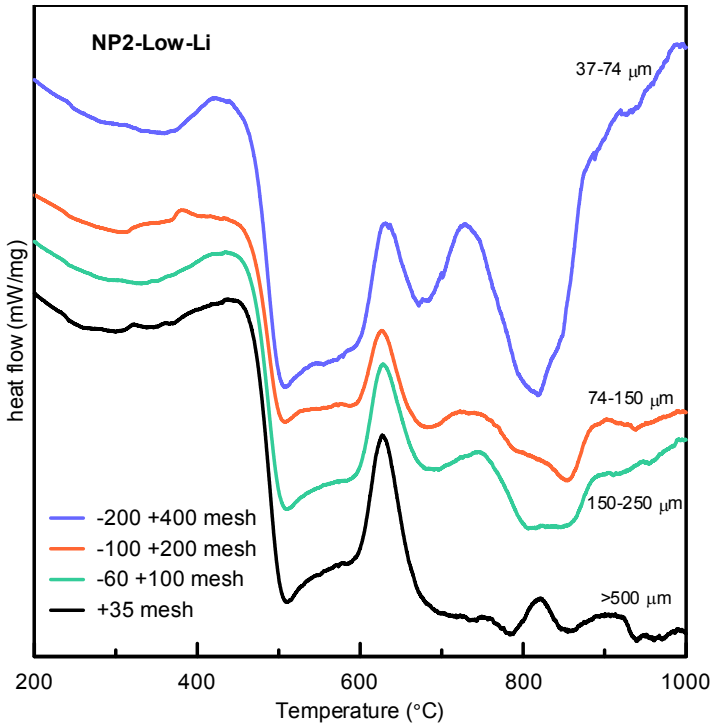

Figure 12. Baseline DSC curves for NP2-Low-Li showing the effect of particle size.

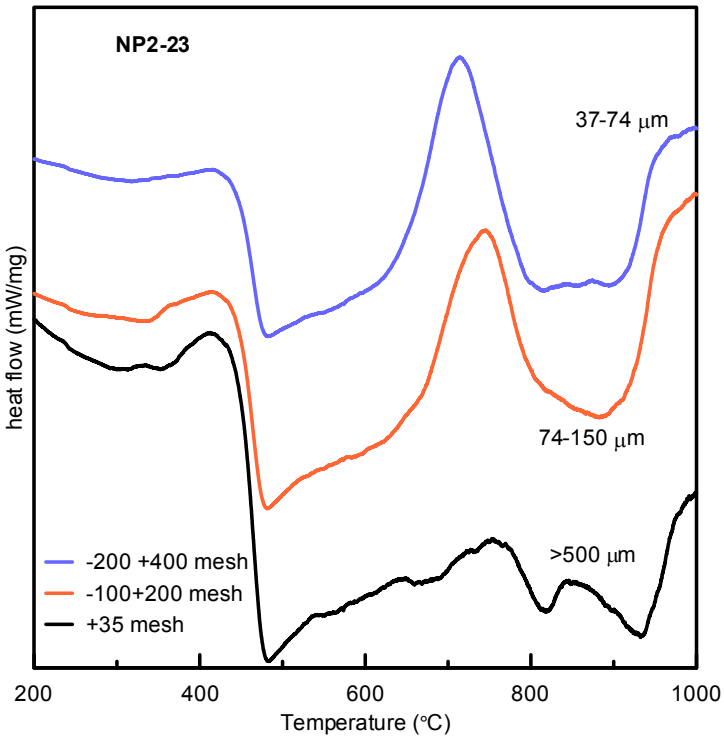

Figure 13. Baseline DSC curves for NP2-23 showing the effect of particle size.

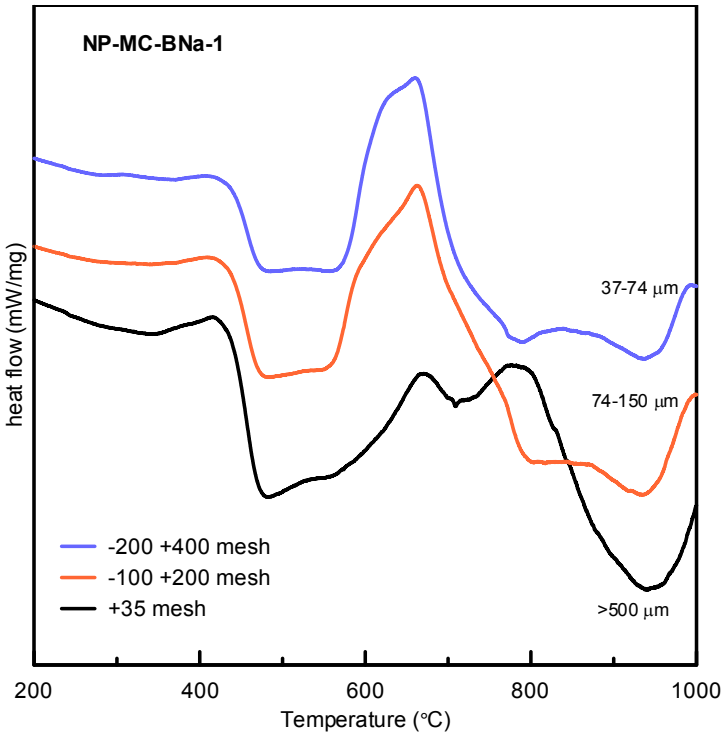

Figure 14. Baseline DSC curves for NP-MC-BNa-1 showing the effect of particle size.

5.0 Conclusions

DSC was used to construct nucleation and crystallization rate curves, as a function of temperature, for three simulated HLW glass compositions. X-ray diffraction of heat treated glasses was used to quantify the crystallization as a function of temperature and agreed well with the derived DSC results. Optical microscopy was used to measure the crystal size as a function of temperature for one of the test glasses (NP2-23). The growth rates regions measured by optical microscopy were comparable to those obtained from XRD, although the growth rate curve measured by optical microscopy was found to occur at a slightly higher temperature, which reflects the real difference in crystal size measurements versus total crystal content. The results of this work demonstrate the feasibility of using DSC to rapidly determine the nepheline growth regions of simulated HLW glasses.

6.0 Future Work

In the next phase of this work, a method will be developed for more directly translating the DSC derived critical temperature region data into crystal growth rates, without the need for confirmation via microscopy or XRD. This will allow for rapidly generated DSC data from a range of glass compositions to be used in estimating the volume fraction of nepheline formed in a canister by combination with heat transfer modeling. In addition, further investigation is needed on the influence of glass surface interfaces (including glass/glass, glass/air, and glass/canister) to elucidate the driving forces for nepheline crystallization and their relationship to actual processing conditions. Once the volume fraction of nepheline is known, its subsequent impact on durability of the IHLW canister will be determined. This will allow for process control strategies to move away from the overly conservative approach of predicting nepheline formation as a function of canister centerline cooling, to a more realistic representation of actual impacts to glass durability for high aluminum concentration feeds.

7.0 References

1. P. J. Certa, R. D. Adams, G. K. Allen, J. D. Belsher, P. A. Empey, J. H. Foster, T. M. Hohl, R. T. Jasper, R. A. Kirkbride, R. L. Lytle, F. L. Meinert, J. S. Ritari, R. M. Russell, K. R. Seniow, E. B. West, M. N. Wells and L. M. Bergmann, "River Protection Project System Plan," *US Department of Energy Report ORP-11242, Revision 6,* US Department of Energy-Office of River Protection, Richland, WA (2011).

2. K. M. Fox, "Task Technical and Quality Assurance Plan for Hanford Waste Glass Development and Characterization," *US Department of Energy Report SRNL-RP- 2013-00692, Revision 1*, Savannah River National Laboratory, Aiken, SC (2016).

3. "Standard Test Methods for Determining Chemical Durability of Nuclear, Hazardous, and Mixed Waste Glasses and Multiphase Glass Ceramics: The Product Consistency Test (PCT)," *ASTM C-1285-02* (2002).

4. C. M. Jantzen and D. F. Bickford, "Leaching of Devitrified Glass Containing Simulated SRP Nuclear Waste," pp. 135-146 in *Sci. Basis for Nuclear Waste Management*, *Vol. 8*, J. A. Stone and R. C. Ewing, eds., Materials Research Society, Pittsburgh, PA, (1985).

5. D. S. Kim, D. K. Peeler and P. Hrma, "Effect of Crystallization on the Chemical Durability of Simulated Nuclear Waste Glasses," pp. 177-185 in Ceram. Trans., Vol. 61, *Environmental Issues and Waste Management Technologies in the Ceramic and Nuclear Industries*, Edited by V. Jain and R. Palmer, The American Ceramic Society, Westerville, OH, 1995.

6. M. R. Kesterson, "COMSOL Multiphysics Model for HLW Canister Filling," *US Department of Energy Report SRNL-STI-2015-00207 Revision 0,* Savannah River National Laboratory, Aiken, SC (2016).

7. J. O. Kroll, J. D. Vienna, M. J. Schweiger, G. F. Piepel and S. K. Cooley, "Results from Phase 1, 2, and 3 Studies on Nepheline Formation in High-Level Waste Glasses Containing High Concentrations of Alumina," *U.S. Department of Energy Report PNNL-26057, EWG-RPT-011,* Pacific Northwest National Laboratory, Richland, Washington (2016).

8. J. W. Amoroso, "The Impact of Kinetics on Nepheline Formation in Nuclear Waste Glasses," *US Department of Energy Report SRNL-STI-2011-00051,* Savannah River National Laboratory, Aiken, SC (2011).

9. A. Marotta, A. Buri and F. Branda, "Nucleation in glass and differential thermal analysis," *Journal of Materials Science*, **16** pp. 341-344, (1981).

10. C. S. Ray, K. S. Ranasinghe and D. E. Day, "Determining crystal growth rate-type of curves in glasses by differential thermal analysis," *Solid State Sciences*, **3** pp. 727-732, (2001).

11. K. Matusita and S. Sakka, "Kinetic Study on Non-Isothermal Crystallization of Glass by Thermal Analysis," *Bull. Inst. Hem. Res., Kyoto University*, **59** [3] pp. (1981).

Appendix A. Quantitative XRD results from isothermal heat treatments of bulk glasses.

Glass ID	Heat Treatment Temperature (°C)	Wt. % Crystalline Phase		
		Nepheline	Lithium Manganese Iron Oxide	Li_2SiO_3*
NP2-23	585	7.4	1.5	0.0
	605	12.4	3.7	1.9
	645	24.6	1.5	3.4
	684	19.1	0.9	1.9
	716	19.2	2.2	0.0
NP2-Low-Li	566	0.0	1.8	
	615	1.7	2.9	
	646	15.6	3.6	
	674	18.2	3.1	
	705	16.8	2.9	
	745	13.2	2.5	
	775	9.8	2.6	
	806	6.0	2.9	
NP-MC-BNa-1	550	15.5	4.6	
	590	34.5	6.1	
	611	37.2	6	
	655	33.7	5.7	
	704	31.8	5.9	

*Li_2SiO_3 was not detected in either the NP2-Low-Li or the NP-MC-BNa1 glasses.

Distribution:

J. W. Amoroso, 999-W
T. B. Brown, 773-A
A. S. Choi, 999-W
Y. S. Chou, PNNL
A. D. Cozzi, 999-W
C. L. Crawford, 773-42A
J. V. Crum, PNNL
D. E. Dooley, 999-W
W. C. Eaton, PNNL
A. P. Fellinger. 773-42A
S. D. Fink, 773-A
K. M. Fox, 999-W
E. K. Hansen, 999-W
C. C. Herman, 773-A
C. M. Jantzen, 773-A
F. C. Johnson, 999-W
D. S. Kim, PNNL
J. O. Kroll, PNNL
A. A. Kruger, DOE-ORP
D. J. McCabe, 773-42A
D. L. McClane, 999-W
D. K. Peeler, PNNL
F. M. Pennebaker, 773-42A
M. J. Schweiger, PNNL
M. E. Stone, 999-W
C. L. Trivelpiece, 999-W
J. D. Vienna, PNNL
W. R. Wilmarth, 773-A
Records Administration (EDWS)